The variability spectrum of ecological communities: How common and rare species shape stability patterns

Jean-François Arnoldi[1,*], Michel Loreau[1], and Bart Haegeman[1] [1]

[1] *Centre for Biodiversity Theory and Modelling, Theoretical and Experimental Ecology Station, CNRS and Paul Sabatier University, 09200 Moulis, France.*

[*]jean-francois.arnoldi@sete.cnrs.fr

September 30, 2018

Abstract

Our empirical knowledge of ecosystem stability and of diversity-stability relationships is mostly built on the analysis of temporal variability of population and ecosystem properties. Variability, however, often depends on external factors that act as disturbances, making it difficult to compare its value across systems, and relate it to other stability concepts. Here we show how variability, when seen as a response to stochastic perturbations of various types, can reveal inherent stability properties of ecological communities, with clear connections with other stability measures. This requires abandoning one-dimensional representations of stability, in which a single variability measurement is taken as a proxy for how stable a system is, and instead consider the whole *variability spectrum*, i.e. the distribution of the system's response to the vast set of perturbations that can generate variability. In species-rich model communities, we show that there exist generic patterns for which specific abundance classes of species govern variability. In particular, the response to stochastic immigration is typically governed by rare species while common species drive the response to environmental perturbations. We show that the contrasting contributions of different species abundance classes can be responsible for opposite diversity-stability patterns. More generally, our work proposes that a multidimensional perspective on stability allows one to better appreciate the dynamical richness of ecosystems, and to better understand the causes and consequences of their stability patterns.

Keywords: ecological stability, demographic stochasticity, environmental stochasticity, rare species, common species, diversity measures, disordered systems, asymptotic resilience.

Introduction

Ecological stability is a notoriously elusive and multifaceted concept (Pimm, 1984; Donohue et al., 2016). At the same time, understanding its drivers and relationship with biodiversity is a fundamental, pressing, yet enduring challenge for ecology (Elton, 1946; MacArthur, 1955; May, 1973; McCann, 2000). Temporal variability (with lower variability being interpreted as a higher stability) is an attractive facet of ecological stability, for several notable reasons. First, variability is empirically accessible using simple time-series statistics such as variance and coefficient of variation (Tilman et al., 1996; Yachi and Loreau, 1999). Second, variability – or its inverse, invariability – is a flexible notion that can be applied across levels of biological organization (Haegeman et al., 2016) and spatial scales (Wang and Loreau, 2014; Wang et al., 2017). Third, variability is indicative of the risk that an ecological system might go extinct, collapse or experience a regime shift (Scheffer et al., 2009). During the last decade, the relationship between biodiversity and ecological stability has thus been extensively studied empirically by focusing on the temporal variability of populations or ecosystem properties (Tilman et al., 2006; Jiang and Pu, 2009; Hector et al., 2010; Campbell et al., 2011; Loreau and de Mazancourt, 2013).

In the literal sense, stability is the property of what tends to remain unchanged (Pimm, 1991). Variability denotes the tendency of a variable to change in time, so that its inverse, invariability, fits this intuitive definition of stability. However, variability is not necessarily an inherent property of the system that is observed (e.g., a community of species), as it typically also depends on external factors that act as perturbations, and generate the observed variability. In other words, the variability of an ecological community is not a property of that community *alone*. It may be caused by a particular perturbation regime (e.g. temperature fluctuations), and a different perturbation regime (e.g. precipitation fluctuations) would lead

to a different value of variability. Stronger perturbations will generate larger fluctuations, and the way a perturbation's intensity is distributed and correlated across species is also critical. As schematically represented in Fig. 1B, a variability measurement reflects the response of a system to the specific environmental context in which it is embedded.

That being said, quantifying the fluctuations of, e.g., primary production of an ecosystem can be of foremost practical interest (Griffin et al., 2009), as it provides – in a given environmental context – a measure of its predictability. However, to generalize results beyond the specific context in which variability is measured, use variability to compare the stability of different systems, establish links between different stability notions, or reconcile the conflicting diversity-stability patterns and predictions reported in the empirical and theoretical literature (Ives and Carpenter, 2007), one needs to know how variability measurements can reflect a system's inherent dynamical properties.

To do so, we adopt an approach in which stability is viewed as the inherent ability of a dynamical system to endure perturbations (Fig. 1A). As a consequence, a measure of stability should not be associated with a particular perturbation (as in Fig. 1B), but instead should reflect a system's propensity to withstand perturbations *in general*.

We consider a vast range of possible perturbations that can generate variability, and study, instead of a unique measure, the corresponding broad range of community responses, which we call *variability spectrum* (Fig. 1C). Even from a theoretical perspective, considering all possible perturbations that any ecological community can face is a daunting task. More prosaically, we will restrict to communities perturbed near equilibrium by weak stochastic perturbations, and derive analytical formulas for two statistical properties of their variability spectrum: its average value (mean-case scenario) and its largest value (worst-case scenario).

We then apply this framework to species-rich model communities subject to different perturbation types (environmental, demographic, or caused by stochastic immigration), and

show that there exist generic patterns for which specific species abundance class govern the variability spectrum. In particular, we demonstrate that there is a generic link between rare species, worst-case variability, and asymptotic resilience – the long-term rate of return to equilibrium following a pulse perturbation. We then explore the role of these patterns in determining diversity-stability relationships. We find that the contrasting contributions of various species abundance classes can be responsible for opposite diversity-stability patterns, probing different dynamical properties of complex communities.

In a nutshell, the goal of our work is (i) to demonstrate that variability is an inherently multidimensional notion, reflecting the multidimensionality of ecosystem's responses to perturbations; (ii) to show that clear patterns exist within ecosystem responses to perturbations reflecting the dynamical properties of distinct species abundance classes; (iii) to argue that, in order to compare and predict stability patterns, it is paramount to first identify to which abundance class these patterns or predictions refer to; and finally, (iv) to propose that a multidimensional perspective on stability allows one to better appreciate the dynamical richness of ecosystems, and the underlying meaning of their stability patterns.

Conceptual framework

To make the schematic representation of Fig. 1 more concrete, we will restrict to the mathematically convenient setting of communities modeled as dynamical systems close to an equilibrium, and study their responses to a whole class of stochastic white-noise forcing. In this section we outline the theory, focusing on ecological intuitions, while Appendix A through D provides a self-contained presentation of its mathematical foundations.

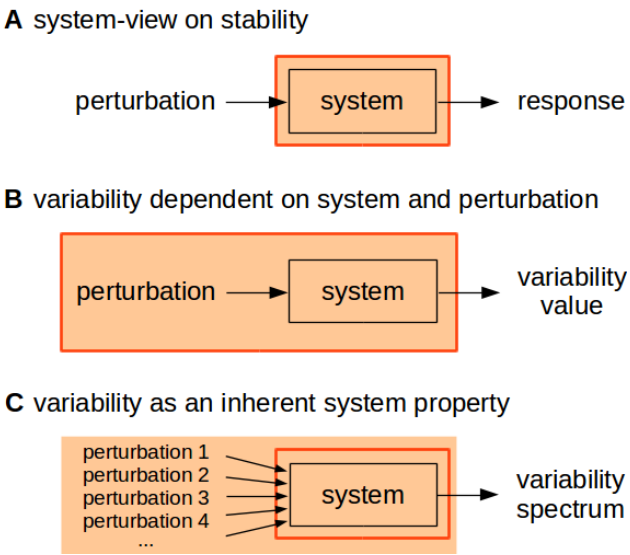

Figure 1: Variability vs stability. A: Stability quantifies the way a system responds to perturbations, seen as an inherent property of the system (indicated by the red framed box). B: By contrast, temporal variability is typically a feature of both the system studied and external factors that act as perturbations. C: For variability to measure the stability of the system, one can consider a whole set of perturbations, thus integrating out the dependence on specific external factors. Here we analyze the patterns that emerge from this approach.

Perturbed communities

Consider a community of S interacting species whose biomass are modeled as continuous interacting dynamical variables $N_i(t)$ approaching an equilibrium value $N_i > 0$, with $i = 1, 2, ...S$. Let $x_i(t) = N_i(t) - N_i$ denote the difference between species i's biomass $N_i(t)$ at time t, and its equilibrium value N_i. We model biomass fluctuations (hence variability) as a response to weak stochastic forcing. We focus on stationary fluctuations caused by perturbations with zero mean, implying that the mean of species time-series correspond to their equilibrium value. From the perspective of any focal species i, the dynamics read

$$\frac{d}{dt} \underbrace{x_i(t)}_{\text{fluctuations}} = \sum_{j=1}^{S} \underbrace{A_{ij} x_j(t)}_{\text{interactions}} + \underbrace{\sigma_i N_i^{\frac{\alpha}{2}} W_i(t)}_{\text{perturbations}}. \tag{1}$$

The coefficients A_{ij} represent the effect that a small change in biomass of species j has on the biomass of species i. Organized in the *community matrix* $A = (A_{ij})$, they encode the linearized dynamics near equilibrium of the non-linear model that has lead to (N_i). The perturbation term,

$$\sigma_i N_i^{\frac{\alpha}{2}} W_i(t), \tag{2}$$

is a stochastic function of time, with $W_i(t)$ denoting a standard white-noise source (Van Kampen, 1997). In discrete time $W_i(t)$ would be a normally distributed random variable with zero mean and unit variance, drawn independently at each time step (Appendix A). We thus assume no temporal autocorrelations of perturbations, i.e., no memory of past events. Although environmental perturbations often follow temporal patterns (Vasseur and Yodzis, 2004; Ruokolainen and Fowler, 2008), the absence of temporal autocorrelation is not a critical assumption for what follows. We will allow, however, for temporal correlations between $W_i(t)$ and $W_j(t)$, which could model a situation in which individuals of species i and j are similar in

their perception of a given perturbation. The perturbation term (2), representing the direct effect that a perturbation has on the biomass of species i, is written as some power of N_i, and is proportional to a species-specific term $\sigma_i W_i(t)$. The latter is a function of the perturbation itself, and of traits of species i which determine how individuals of that species perceive the perturbation. We will discuss this term in detail in following sections.

Not all dynamical systems written as (1) lead to stationary fluctuations. For this to be the case, the equilibrium must be stable. More technically, the community matrix A must satisfy the stability criterion: all its eigenvalues must have negative real part (May, 1973; Gurney and Nisbet, 1998). The eigenvalue with maximal real part determines the slowest long-term rate of return to equilibrium following any weak pulse perturbation. This rate is a commonly used stability measure in theoretical studies. We call it *asymptotic resilience* and denote it by $\mathcal{R}_\infty$ (Arnoldi et al., 2016*b*). It will serve as a reference.

Perturbation type

The dependency with species biomass of the perturbation term (2) models a statistical relationship between a perturbation's direct effects and the mean biomass of perturbed species. This relationship allows to consider many, and very distinct, sources of variability (Fig. 2).

When individuals of a given species respond in synchrony to a perturbation, its direct effect will scale roughly linearly with the abundance of that species, thus a value of α in eq. (2), close to 2. We call this type of perturbation *environmental* as fluctuations of environmental variables typically affect all individuals of a given species, leading, for instance, to changes in population growth rate (Lande et al., 2003). If individuals respond incoherently, however, e.g., some negatively and some positively, the direct effect of the perturbation on that species biomass will scale sublinearly with that species abundance. For instance, demo-

graphic stochasticity can be seen as a perturbation resulting from the inherent stochasticity of birth and death events, which are typically assumed independent between individuals. In this case $\alpha = 1$, and we call such type *demographic* (Haegeman and Loreau, 2011). The power-law relationship can also encode purely exogenous perturbations, such as the random removal or addition of individuals. This can be done by setting $\alpha = 0$. We call the latter of the *immigration* type but stress that actual immigration events are not necessarily of this type (e.g. they can be density-dependent).

With the expression (2) we can thus consider a continuum of perturbation type, from purely exogenous stochasticity (immigration-type $\alpha = 0$), to environmental perturbations ($\alpha = 2$), via demographic stochasticity ($\alpha = 1$). Although not unrelated, the statistical relationship (2) between a perturbation's direct effects and the biomass of perturbed species is not equivalent to Taylor's (1961) law. The latter is an empirically observed power-law relationship between variance and mean of population biomass time-series. We will come back to this point in the Discussion.

Community response vs perturbation intensity

For a given community, a stronger perturbation will naturally lead to stronger fluctuations. This could reveal non-linear dynamical properties of the system considered, but in a linear setting, by definition, this is not the case. Since we placed ourselves in this setting, to see in temporal variability a reflection of a community's dynamical properties, we must control for perturbation intensity. We now discuss how to do so, for a simple definition of variability.

By linearity, the fluctuations induced by white-noise forcing are normally distributed, thus fully characterized by their variance and covariance. It thus makes sense to construct a measure of variability based on the variance of species biomass. To allow a comparison between

communities of different diversity, a simple choice is to consider the average variance,

$$\sigma^2_{\text{out}} = \frac{1}{S}\sum_i \text{Var}(N_i(t)). \tag{3}$$

We will discuss this choice further, but for now, from this definition of community response, we wish to remove the trivial effect of perturbation intensity. Let us start from a one-dimensional system $dx/dt = -rx + \sigma W(t)$. Its stationary variance is $\sigma^2_{\text{out}} = \frac{\sigma^2}{2r}$. We see here the contribution of perturbation σ^2 and dynamics r in determining the response. Here, a natural choice for perturbation intensity is σ^2. For species-rich communities, if we define the intensity of a perturbation as the average intensity felt by species thus, from eq. (2),

$$\sigma^2_{\text{in}} = \frac{1}{S}\sum_i \sigma_i^2, \tag{4}$$

then the maximal community response will be proportional to the perturbation's intensity. To remove this trivial dependency from our measure of variability, we consider the ratio

$$\mathcal{V} = \sigma^2_{\text{out}}/\sigma^2_{\text{in}}, \tag{5}$$

from which we deduce a measure of stability, *invariability*, defined as

$$\mathcal{I} = 1/2\mathcal{V}. \tag{6}$$

The factor 1/2 in the definition of invariability allows it to coincide, for simple systems, with asymptotic resilience. It is the case for the one-dimensional example considered above, where $\mathcal{R}_\infty = r$ and, in response to immigration-type perturbations, $\mathcal{V} = 1/2r$, so that $\mathcal{I} = r = \mathcal{R}_\infty$.

In empirical studies, temporal variability is often associated to a given observable ecosys-

tem function (primary productivity, respiration, basal or top species biomass, and so forth). In our setting, this amounts to measuring the ecosystem response along a direction in the space of dynamical variables. In Appendix B we explain considering average variance to define variability, amounts to taking the expected variance along a random choice of direction of observation. In this sense, eq. (3) represents a "typical" observation. We will come back in the Discussion (and Appendix I) to other variability metrics that have been used in empirical studies, such as coefficient of variation of total biomass or populations.

Variability spectra

Once intensity is controlled for, perturbations can still differ in how their intensity is distributed and correlated across species. For example, we want to be able to model the fact that species with similar physiological traits ought to be affected in similar ways by, say, temperature fluctuations, whereas individuals from dissimilar species may react in unrelated, or even opposite, ways. We will thus study the effect of changing the covariance structures of the perturbation terms, at fixed intensity. In this sense, any perturbation of a given type has a "direction" encoding the way its intensity is distributed across species, but also encoding the temporal correlations between its direct effects on species. Unlike changing overall intensity, considering different directions allows to probe different dynamical properties of a same community.

For a given community, spanning the set of all perturbation directions will naturally define a whole range of responses. Assuming some probability distribution over this set consequently defines a probability distribution over the ensuing responses. We call this latter distribution the *variability spectrum*, illustrated in Fig. 2. We will typically assume all perturbation directions to be equiprobable, but our framework allows different choices of prior. Furthermore,

spanning the set of perturbation types then reveals a continuous family of *variability spectra* (blue, green, and red distributions in Fig. 2).

For each spectrum we will consider two complementary statistics, namely mean- and worst-case responses. In Appendix C we prove that the worst-case response is always achieved by a perfectly coherent perturbation, i.e., a perturbation whose direct effects on species are not independent, but on the contrary, perfectly correlated in time. We give an explicit formula (see eqs. (C3-D6)) to compute the worst-case from the community matrix and species equilibrium biomasses. The mean-case scenario is defined with respect to the prior probability distribution over the set of perturbation directions. In the case of a uniform distribution (i.e. equiprobable directions, the least informative prior), we prove in Appendix C that a perturbation affecting all species independently but with equal intensity is met with the mean-case response. This yields a simple formula to compute the mean case directly from the community matrix and species equilibrium biomasses, see eqs. (C4-D7).

Variability spectra of a two-species community

Before moving on towards more complex communities, let us illustrate our variability framework on the following elementary example, in the form of a 2×2 community matrix

$$A = \begin{pmatrix} -1 & 0.1 \\ -4 & -1 \end{pmatrix} \tag{7}$$

This matrix defines a dynamical system that could represent a predator-prey community, with the first species benefiting from the second at the latter's expense. It is stable with asymptotic resilience $\mathcal{R}_\infty = 1$. Let us suppose that the biomass of the prey, N_2 (second row of A) is 7.5 times larger than the one of its predator, N_1 (first row of A) and consider

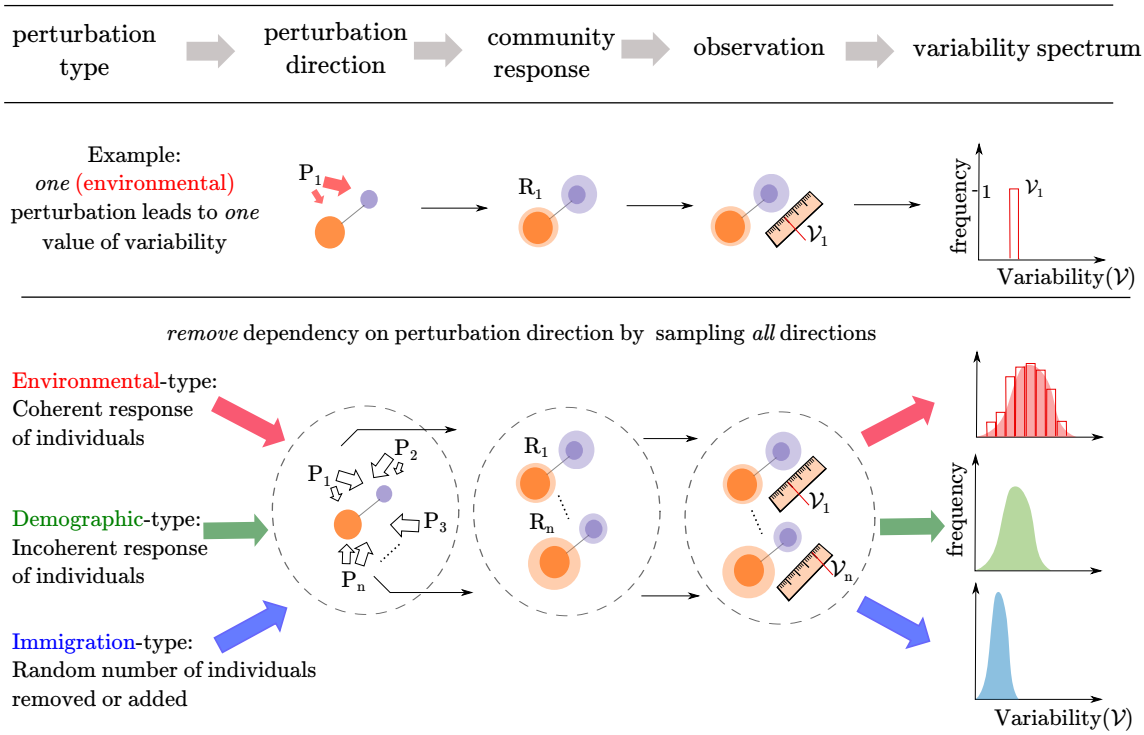

Figure 2: The variability spectrum as a function of perturbations type. Top row: as previously illustrated in Fig. 1B, a variability measurement of a community (here two species, represented by the orange and purple discs, whose diameter represent abundance) is a function of both the dynamics of this community and the environmental perturbation P_1 that it faces. Subsequent rows: we will consider various types of perturbations ranging from environmental to immigration, via demographic stochasticity (see main text for a precise definition). We eliminate the dependence on specific features of perturbations (i.e. their direction, see main text) by sampling many perturbations leading to a whole spectrum of response, called the variability spectrum. Considering all types of perturbations then reveals, for a given system, a family of variability spectra. This gives an extensive characterization of the system's stability.

stochastic perturbations of this community, as formalized in eq. (1).

In Fig. 3 we represent, for any given type, the set of perturbation directions as a disc, every point of the disc corresponding to a unique perturbation direction (see Appendix E for details). The effect of a perturbation on a community can be represented as a color, darker tones implying larger response, with the baseline color (blue, green or red) recalling the perturbation type ($\alpha = 0, 1, 2$, respectively). Points at the borders of the discs correspond to perfectly correlated perturbations, so that the largest response is achieved from such perturbations: the color maps represented in Fig. 3 which are always darkest on the borders of the disc.

We see in the second row of Fig. 3 that variability not only depends on the perturbation directions, but that this dependence is in turn strongly affected by the perturbation type. For immigration-type perturbations (in blue) variability is largest when perturbing the predator species most strongly (the least abundant species in this example). For demographic-type perturbations (in green) perturbations that equally affect the two species but in opposite ways achieve the largest variability. For environmental-type perturbations (in red) variability is largest when perturbing the prey species (the most abundant species in this example). For all types we see that positive correlations between the components of the perturbation (moving upwards on the disc) reduce variability.

This example confirms that, in general, a given community cannot be associated to a single value of variability, even if the intensity and type of perturbation is fixed. Importantly, depending on the origin of perturbations causing variability, different species can have completely different contributions to variability. This stands in sharp contrast with asymptotic resilience which associates a single stability value to the community. Note that it is unclear at this stage how the different species contribute to asymptotic resilience.

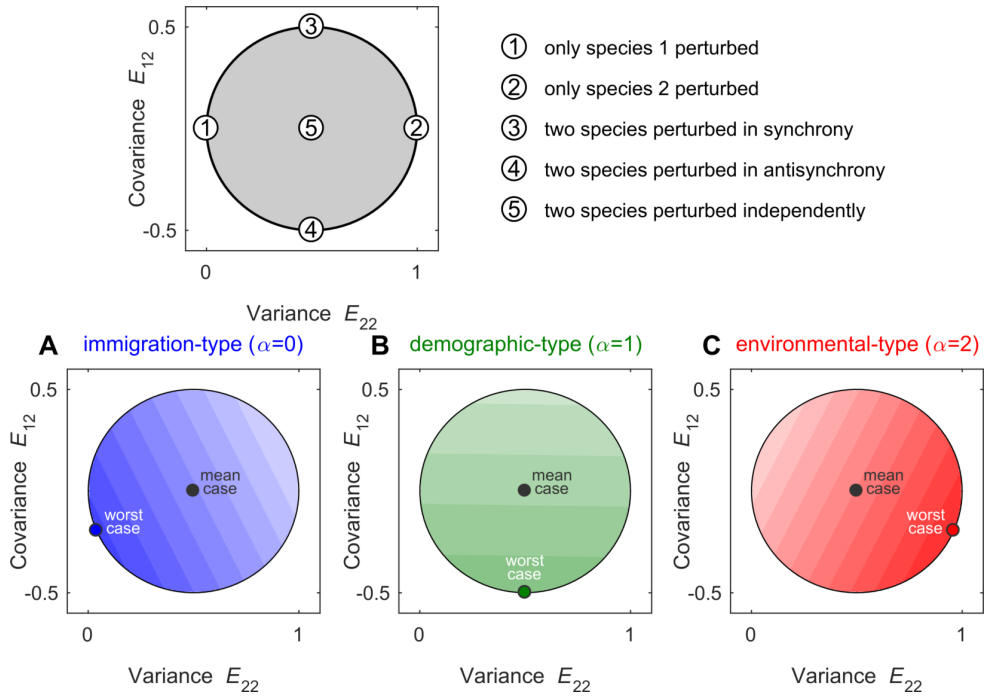

Figure 3: Variability depends on perturbation direction and perturbation type. Top panel: For a two-species community the set of all perturbation directions can be represented graphically as a disc (shaded in gray), with the variance of the perturbation term $\xi_2(t)$ on the x-axis and the covariance between $\xi_1(t)$ and $\xi_2(t)$ on the y-axis. Some special perturbation directions are indicated (numbers 1 to 5, see also Appendix E). Panels A–C: We consider a predator-prey system; the community matrix A is given by eq. (7), and the equilibrium biomass for the predator (species 1) is 7.5 times smaller than for the prey (species 2). The induced variability depends on the perturbation directions (darker colors indicate larger variability), and this dependence in turn depends on the perturbation type α. A: For immigration-type perturbations ($\alpha = 0$, in blue) variability is largest when perturbing species 1 most strongly. B: For demographic-type perturbations ($\alpha = 1$, in green) perturbations that affect the two species equally strongly but in opposite ways achieve the largest variability. C: For environmental-type perturbations ($\alpha = 2$, in red) variability is largest when perturbing species 2 most strongly. Notice that the worst case is always achieved by perturbations lying on the edge of the perturbation set. Such perturbations are fully correlated (see main text and Appendix E).

Stability patterns of complex communities

As we now argue, the concept of variability spectra becomes particularly relevant when considering communities comprised of many species in interaction. To generate such communities, we consider a pool of species following random Lotka-Volterra interactions and let the dynamics settle to a realized equilibrium community. By drawing random growth and interaction parameters we generate many stable communities of various complexity (see Appendix F for details). Importantly, such communities exhibit uneven abundance distributions, thus allowing perturbation types to play an important role in a community's variability.

In species-rich communities the perturbation set cannot be represented as in the two-dimensional example of Fig. 3. What is possible and enlightening, however, is to focus on the effect of a specific subset of perturbations, those that affect a single species. By superposition, this allows the study of perturbation scenarios in which species are affected independently, but it excludes scenarios in which species are perturbed in systematically correlated or anti-correlated way. In Fig. 4 we consider a random community of 40 interacting species. We order species according to their abundance and plot the variability induced by perturbing them. We observe the following, clearly identifiable patterns:

(i) When caused by immigration-type perturbations, variability is inversely proportional to the abundance of the perturbed species (leftmost panel). In other words, randomly adding and removing individuals from common species generates less variability than when the perturbed species is rare. In fact, the worst-case scenario corresponds to perturbing the rarest species. Remarkably, worst-case invariability remains close to asymptotic resilience, which corroborates previous findings that showed that asymptotic resilience is often associated to rare species, pushed towards extinction by the rest of the community (Haegeman et al., 2016; Arnoldi et al., 2018). (ii) When caused by demographic-type perturbations, variability seems

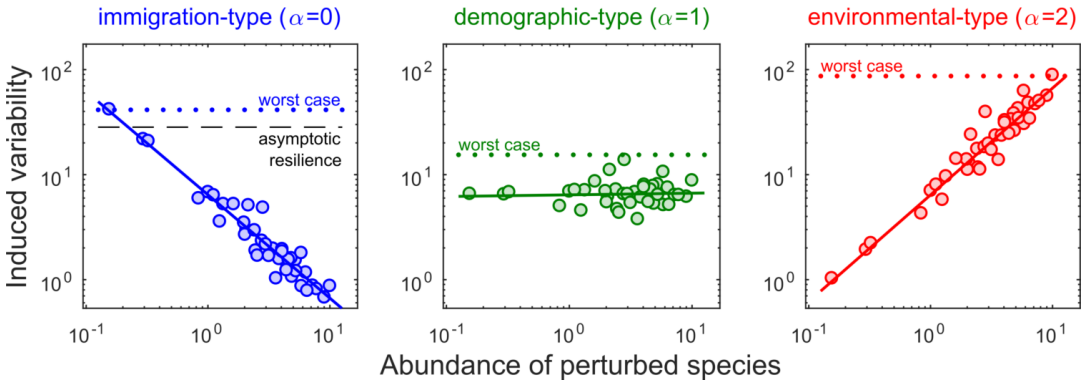

Figure 4: The contribution of abundant and rare species to variability. We consider a community of $S = 40$ species, and look at the variability induced by perturbing a single species, whose abundnace is reported on the x-axis. Left: When caused by immigration-type perturbations ($\alpha = 0$), variability is inversely proportional to the abundance of the perturbed species (notice the log scales on both axis). The worst case is achieved by perturbing the rarest species, and is determined by asymptotic resilience (more precisely, it is close to $1/2\mathcal{R}_\infty$). Middle: For demographic-type perturbations ($\alpha = 1$), variability is independent of the abundance of the perturbed species. The worst case is not necessarily achieved by focusing the perturbation on one particular species. Right: For environmental-type perturbations ($\alpha = 2$), variability is directly proportional to the abundance of the perturbed species. The worst case is attained by perturbing the most abundant one.

to be unrelated to the abundance of the perturbed species (middle panel). (iii) When caused by environmental-type perturbations, variability is proportional to the abundance of the perturbed species (rightmost panel). In this case, despite being more stable than rare ones, common species are more strongly affected by environmental perturbations, allowing them to dominate variability.

It is importnat to realize that the patterns reported in Fig. 4 are not self-evident but emerge from interactions between species. In their absence, the response to a perturbation of a given species involves only that species, and is entirely driven by its growth rate r. The relationship between variability $\mathcal{V}$ and the perturbed species abundance N is, in this case,

$\mathcal{V} = N^{\alpha}/2r$, where N coincides with the carrying capacity K of that species, and α indexes the perturbation type. Thus, without interactions there is no reason to expect the patterns reported in Fig. 4. This is illustrated in the top left panel of Fig. 5. Moreover, if there is a r vs K trade-off, abundant species would be the least stable ones and drive variability patterns regardless of its type (Fig. 5, bottom left panel). However, as interaction strength increases (panels from left to right in Fig. 5), we see emerging the relationship between abundance and variability described in Fig. 4, showcasing its genericity. In Appendix G we explain why this reflects a limit-case behavior for so-called disordered communities (Barbier et al., 2018; Bunin, 2017) in which equilibrium abundances of species are hardly determined by their own carrying capacities, but mostly by direct and indirect effects with others species, indicating a high degree of collective integration in the community.

Implications for the diversity-stability relationship

Let us now explore the underlying role of the above patterns in diversity-stability relationships.

By gradually increasing the size of the species pool and drawing random growth and interaction parameters, we generate many different communities of various diversity from the same class of random Lotka-Volterra models as above. For every community we compute the bulk of its variability spectra (10th to 90th percentiles responses to uniformly drawn perturbations) together with mean- and worst-case scenarios, as well as asymptotic resilience.

In the leftmost panel of Fig. 6, stability *sensu* invariability, eq. (6), is defined from the response to immigration-type perturbations. It is an exponentially decreasing function of diversity (notice the log scale on the y-axis). Asymptotic resilience and worst-case invariability mostly coincide, with a decreasing rate roughly twice as large as the one of the mean case. Here, clearly, diversity begets instability (May, 1972). In the middle panel, defining stabil-

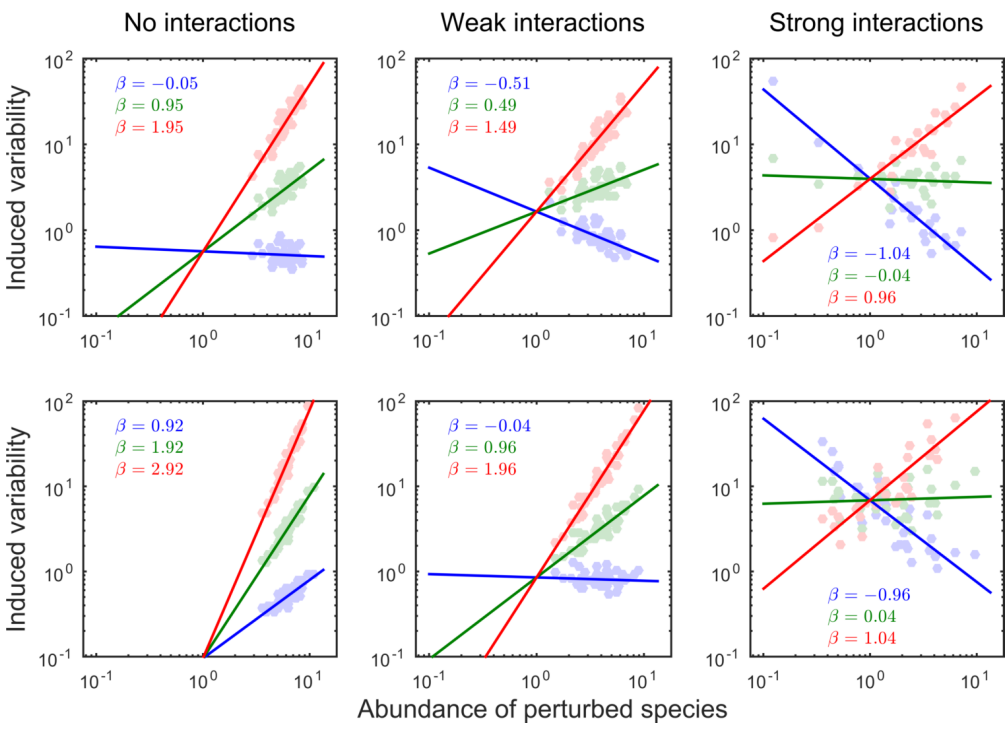

Figure 5: The emergence of the role of species abundance in a community's variability (as in Fig. 4: one species perturbed at a time, with is abundance on the x-axis). Top row: intrinsic growth rates r and carrying capacities K are sampled independently. Bottom row: Species satisfy a r vs K trade-off. Colors correspond to the three perturbation types: $\alpha = 0$ (blue), $\alpha = 1$ (green) and $\alpha = 2$ (red). The value β reported in each panel corresponds to the exponent of the fitted relationship $V_i \propto N_i^{\beta}$ for each perturbation type. As interaction strength increases (left to right) we see emerging the relationship between abundance and variability described in Fig. 4, i.e., $\beta = \alpha - 1$. Thus when species interactions are sufficiently strong, variability always ends up being: (blue) inversely proportional, (green) independent and (red) directly proportional to the abundance of the perturbed species.

ity from the response to demographic-type perturbations gives a different story. Mean-case invariability stays more or less constant whereas the worst-case diminishes at an exponential rate with diversity. The rate of decrease is however four times smaller then of asymptotic resilience. Here the relationship between diversity and stability appears to be ambiguous. Finally, in the rightmost panel, environmental perturbations yield an increase of all realized invariability values with diversity, in sharp contrast with the trend followed by asymptotic resilience.

The spread of biomass across more and more species along the diversity gradient has thus opposite effects on variability depending on the type of perturbation causing it. In the case of immigration-type perturbations, the increasing rarity of many species is a source of instability. Assuming interactions are not rapidly reduced by diversity, the limit of relatively strong interactions described in Figs. 4 and 5 is the one towards which a community of increasing diversity will tend. Thus, at high enough diversity each species contributes to variability proportionally to the inverse of its abundance so that the worst case scenario follows the abundance of the rarest species, which rapidly declines with diversity. Furthermore, as detailed in Appendix H, mean-case invariability will scale as an average abundance which typically decreases with diversity. In response to environmental-type perturbations, it is now abundant species that mostly contribute to variability with the worst-case scenario following the abundance of the most common species. Mean-case variability (and not its inverse) now scales as an average abundance. Here the number of rare species matters for mean-case variability but not their individual abundance.

There is thus close connection between stability and diversity metrics. As has been said about diversity metrics (species richness, Simpson index or Shannon entropy), different invariability measures "differ in their propensity to include or to exclude the relatively rarer species" (Hill, 1973). In this sense, they probe different dynamical aspects of a same community, with

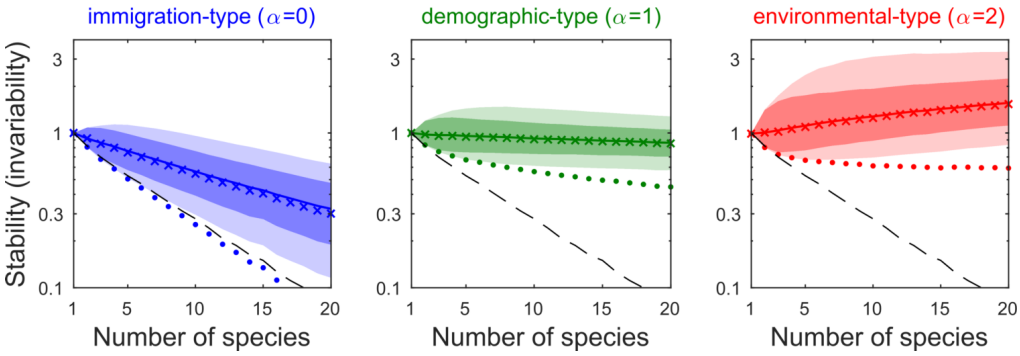

Figure 6: Different perturbation types yield contrasting diversity-stability relationships. We generated random Lotka-Volterra competitive communities of increasing diversity and computed their invariability (log scales on both axes). We computed the invariability for 1000 perturbation directions; full line: median over perturbations, dark-shaded region: 5th to 95th percentile, light-shaded region: minimum to maximum realized. The $\times$-marks correspond to the analytical approximation for the median invariability, the dots to the analytical formula for the worst-case invariability. As a reference, the dashed line follows asymptotic resilience along the diversity gradient. For immigration-type perturbations ($\alpha = 0$, blue) diversity begets instability, with asymptotic resilience closely following worst-case invariability. For demographic-type perturbations ($\alpha = 1$, green) mean-case invariability does not vary with diversity. For environmental-type perturbations ($\alpha = 2$, red) stability increases with diversity.

potentially opposite dependencies on a given ecological parameter of interest.

Finnaly, is worth noting that, In all panels of Fig. 6 the bulk of invariability stays close to the mean-case while moving away from the worst-case invariability. This is because the worst-case scenario corresponds to a single direction of perturbation met with the strongest response, i.e., a fine-tuned perturbation exploiting specific dynamical interdependencies between species that ought to become less and less likely to pick at random as diversity increases. The mean-case is by definition more representative of generic perturbations, allowing for compensatory effects between species.

Discussion

Summary of results

Because it is empirically accessible using simple time-series statistics, temporal variability is an attractive facet of ecological stability. Yet there are many ways to define variability in models, or to measure it on data, a proliferation of definitions reminiscent of the proliferation of definitions of stability itself (Grimm and Wissel, 1997). From an empirical perspective, variability measurements often depend, not only on the system of interest, but also on external factors that act as disturbances, which makes it difficult to relate variability to other stability concepts (Donohue et al., 2016). These caveats constitute important obstacles toward a synthetic understanding of ecological stability, and its potential drivers.

Here we proposed to see in variability a reflection of an ecosystem's response to stochastic perturbations. We showed how, in this approach, variability can reveal inherent dynamical properties of ecological communities. We did so not by seeking for an optimal, single measure of variability but, on the contrary, by accounting for a vast set of perturbations that a given community can face. We called the ensuing response distribution the *variability spectrum*. We studied two complementary statistics of the variability spectrum: the worst- and mean-case responses as functions of the abundance, growth rate, and interactions of species and, importantly, of the *type of perturbations*.

A perturbation type characterizes a statistical relationship between its direct effect on a population and the latter's abundance. We distinguished between: (i) environmental perturbations, whose direct effects on populations scales proportionally with their abundance, (ii) demographic perturbations, whose direct effect on populations scales sublinearly with their abundance, and (iii) purely exogenous perturbations, representing random addition and removal of individual independently of the size of the perturbed population (immigration-type).

After controlling for perturbation type and intensity, we considered all the ways this intensity can be distributed and correlated across the species of a community. Since each perturbation type defines a variability spectrum, the notion of variability unfolds as a continuous family of *variability spectra.*

On random Lotka-Volterra community models we found that, depending on perturbation type, both common or rare species can determine variability. This is reminiscent of diversity measures (Hill, 1973): some (e.g. species richness) are sensitive to rare species, while others are mostly indicative of abundant ones (e.g. Simpson diversity index). For a sequence of model communities of increasing species richness, that immigration-type perturbations gives a prominent role to rare species explains the negative diversity-stability observed in Fig. 6. It reflects the growing vulnerability of rare species pushed towards the edge of extinction as diversity increases. Such rare species do not regulate well immigration type perturbations, which leads them to determine the largest values of the variability spectrum. More generally, the contribution of species to variability generically scales as the inverse of their abundance (Fig. 4), which leads to a proportional relationship between mean-case invariability and average abundance, the latter typically declining with diversity (Appendix H). When caused by demographic-type perturbations, a species contribution to variability is generically independent of its abundance, allowing for potentially ambiguous diversity-stability patterns. By contrast, common species are generically the most stable, yet also the most affected by environmental perturbations, allowing them to drive the larger values of the variability spectrum. More generally, the contribution of species to variability is generically proportional to their abundance (Fig. 4) which in turns leads to a proportional relationship between average abundance and mean-case variability (and not its inverse as was the case for immigration-type), typically leading to a positive diversity-stability relationship.

Of the two patterns described – emerging role of abundance and diversity-stability rela-

tionships – the first is the most robust to modeling choices or details of species traits. Indeed, whereas the sign of diversity-stability relationships can depend, amongst other things, on the way interactions change with diversity, the described contributions to variability of species abundances classes reflect a generic outcome of the assembly of disordered systems. As illustrated in Fig. 5 and detailed in Appendix G, the sole requirement is that interactions in a species-rich community are sufficiently strong and heterogeneous.

Our results showcase the fact that variability strongly depends on factors external to the system of interest. There are cases, however, in which this does not constitute a fundamental problem. When approaching a regime shift, early warning signals based on variability are generically independent of the perturbation or of the way that the response is observed (Scheffer et al., 2009). This is because when a system approaches a global instability, most perturbations will excite the unstable direction, and most observation will detect it. Similarly, all stability measures should coincide near a catastrophic transition. In the absence or far from such transitions, stability metrics can branch out, as well as possible invariability measurements, and it is in this context that our work ought to be most relevant.

Theoretical consequences

We could relate variability to asymptotic resilience, the most commonly used stability metric in theoretical studies (Donohue et al., 2016). We found that asymptotic resilience is comparable to the largest variability in response to an immigration-type perturbation, which is often a perturbation of the rarest species (first panel of Fig. 4). While the asymptotic rate of return to equilibrium is sometimes considered as a measure representative of the collective recovery dynamics, we recently showed that this is seldom the case (Arnoldi et al., 2018). The asymptotic rate of return often reflects dynamical properties of rare "satellite" species,

pushed at the edge of local extinction by abundant "core" species. By contrast, short-time return rates can exhibit qualitatively different properties related to abundant species. This suggest that the multiple dimensions of variability are related to the multiple dimensions of return times. Indeed, variability reflects a superposition of responses to pulse perturbations, some of which have just occurred and are thus hardly absorbed, while others occurred long ago and are thus largely resorbed. Variability is thus an integral measure of the transient regime following pulse perturbations. If abundant species are faster than rare ones (which, as we showed, is typically the case in complex communities), if they are also more strongly perturbed (e.g. by environmental perturbations), the bulk of the transient regime will be relatively short. Thus variability in response to environmental perturbations is associated with short-term recovery dynamics. By contrast, if all species are, on average, equally displaced by perturbations (e.g. by immigration-type perturbations), rare species initially contribute to the overall community displacement as much as abundant ones, and if they are much slower to recover (which is often the case), the bulk of the transient regime will be longer. Thus variability in response to immigration-type perturbations is associated with the long-term return rate to equilibrium (which converges towards asymptotic resilience).

The link between asymptotic resilience, immigration invariability and rare species, also suggests a connection with the notion of *feasibility*: the probability, for a given set of species, that a coexistence equilibrium exist, where all species have a positive abundance (Roberts, 1974; Grilli et al., 2017). Indeed, in an assembly context there is a continuum from common, to rare, to extinct. If feasibility drops then we can also expect that some species will be rare, and will drive asymptotic resilience and worst-case immigration invariability. In other words, we should expect these three notions (feasibility, asymptotic resilience, worst-case immigration invariability) to go hand in hand in the context of community assembly.

One could think that asymptotic resilience, and thus variability in response to immigration-

type perturbations, should also be closely linked to May's (1972) seminal article predicting a "complexity bound" beyond which most systems are unstable. Indeed, as in many theoretical works since then (e.g. Gross et al., 2009; Allesina and Tang, 2012), stability in May's work referred to the probability of a random community matrix to be stable, thus defining a linear dynamical system with positive asymptotic resilience. In our work, however, we did not rely on the probability of drawing a stable state: starting from a random pool of species, we let community assembly play out to reach an equilibrium, which is stable by construction. This nuance is in an important one (Bunin, 2017). Yet, Biroli et al. (2017) recently revealed a connection between May's work and community assembly, showing that May's bound applies to Lotka-Volterra systems, predicting the diversity limit beyond which the community is in a collective state of marginal stability, or chaos. The growing instability with diversity predicted by May, however, is not to be seen in the asymptotic resilience of assembled communities, but in properties of their per-capita interaction matrix, which is independent of species abundances (see Appendix G). Recall that we found abundances to play no significant role in the response to demographic perturbations (middle panel of Fig. 4). This is because, in disordered communities, demographic variability is also an intrinsic feature of the per-capita interaction matrix (Barbier et al., 2018). Thus the link between May's work and ours is likely to be found in patterns of demographic variability. Furthermore, because the work of Biroli et al. shows that May's bound signals a collective dynamical shift in complex communities, it also suggests that demographic perturbations probe the collective response of ecosystems.

Although these reasonings go beyond the scope of this article, they clearly showcase the potential of the variability spectrum framework to encompass previously disconnected theoretical works on ecological stability.

Empirical consequences

Of the two statistics of the variability spectrum that we studied (i.e. mean- and worst-case variability), only the mean-case scenario is empirically accessible. Ideally it could be reconstructed from multiple observations of a same community under different environmental conditions. However, depending on the question addressed, simpler protocols may be sufficient. For instance, in diversity-stability studies, observing many communities in the same environment (e.g. undergoing a unique perturbation regime) is a way to assess an average response, because the direct effect of a perturbation on the community –its *direction*– depends both on the perturbation itself, and on the way individuals from different species perceive it. Thus, sampling many communities also spans many perturbation directions.

On the other hand, the worst-case scenario corresponds to a theoretical prediction that is unlikely to be observed. The potentially strong discrepancy between mean- and worst-case scenarios implies that the variability spectrum of communities should be expected to be broad, so that differences around an average are not solely caused by observational errors but can reflect the inherent multidimensionality of an ecosystem's response to perturbations.

Variability offers a convenient way to address the stability of ecosystems at different levels of organization. For instance, the coefficient of variation (CV) of total biomass has been used as a measure of stability at the ecosystem level (Tilman et al., 2006; Hector et al., 2010). On the other hand, the weighted average CV of species biomass is typically interpreted as population-level stability. These two variability notions thus differ in the variables observed. By contrast, our approach was to consider, for a given observation scheme, the various responses caused by various types of perturbation. Empirical studies have reported a general tendency for diversity to correlate positively with stability at the ecosystem level, but negatively at the population level (Jiang and Pu, 2009; Campbell et al., 2011). In Appendix I, with

the same model communities used to generate Fig. 6, we corroborate these empirical findings. Instead of defining variability as mean variance, we considered CV-based stability measures, and indeed found ecosystem-level invariability to increase with diversity for all perturbation types, while population-level invariability always decreases (Fig. I1). This can be explained from the fact that, by construction, ecosystem-level stability gives a predominant weight to abundant species, while population-level stability gives a large weight to rare species. Here, underlying the contrasting diversity-stability relationships, is again a contrasting role given to species depending on their abundance, but the difference is now due to the choice of observation itself instead of the perturbation type. This highlights the fact that the role given to species abundance classes, either because of inherent dynamical reasons or due to the choice of observation variable, is a fundamental driver of observed stability patterns.

While it is clear that the choice of observation predetermines the level of organization of interest, that the type of perturbations can also reflect the dynamical properties of distinct species abundance classes is a novel statement that opens the door to empirical investigations. For instance, the physical size of the system considered should affect which perturbation type predominates and thus which species abundance class is most likely to contribute to variability. Suppose that a spatially homogeneous community, say the predator-prey system considered in Fig. 3, is observed at two spatial scales. At the small scale, implying small populations, we can expect variability to be mostly caused by demographic stochasticity. At larger scales, implying larger populations, demographic stochasticity will be negligible compared with environmental perturbations. Just as changing the perturbation type transformed the variability spectra in our simple example presented in Fig. 3, patterns of variability at these two scales will reflect different aspects of the community. Thus, without invoking spatial heterogeneity, there are reasons to expect a non-trivial spatial scaling of stability (Chalcraft, 2013), reflecting an underlying transition of the species abundance classes that contribute to the ecosystem's

dynamical response to the perturbations that it faces.

Empirical testing of these ideas would require determining the type of perturbations affecting a given community. This means estimating the exponent α that characterizes the various perturbation types. This could be done, e.g. by identifying perturbation events and fitting a power-law to their effect on species as a function of the latter's abundance. One could also look for a direct relationship between the exponent α and that of Taylor's (1961) law that links mean and variance of population sizes. In fact Taylor's law is an output of our framework with perturbation type as an input, and thus, ought to affected by species interactions (Kilpatrick and Ives, 2003). It would thus be useful to check whether the simple models of the diversity-stability relationships based on an assumed Taylor's law are consistent with the predictions of our framework.

Conclusion

The multidimensional nature of variability can lead to conflicting predictions but, once acknowledged, can be used to probe the dynamical properties of different species abundance classes within a community, in a similar way as various diversity measures reflect the presence of different species abundance classes. By shifting the focus from a single measure of variability to the variability spectrum, we could more clearly appreciate the dynamical richness of complex systems and demonstrate the impossibility of any one-dimensional characterization of their stability. This applies beyond the technical setting of our work: although we did not consider strong non-linearities, autocorrelation of perturbations or spatial processes, these additional dimensions can also be used to probe and reveal other important dynamical behaviors (Zelnik et al., 2018). This work provides a dialectical perspective on ecological stability. A community is not a mere aggregation of rare and abundant species, as these

species can be rare and abundant as a product of their interactions with the rest of the community. Variability can probe the dynamics at the species level (rare to abundant species) but also of more collective properties. All are intertwined, and reflect important aspects of a community's dynamical identity.

Acknowledgements

We wish to thank Yuval Zelnik for helpful discussions and review of the manuscript, and Matthieu Barbier for helpful discussions. This work was supported by the TULIP Laboratory of Excellence (ANR-10-LABX-41) and by the BIOSTASES Advanced Grant, funded by the European Research Council under the European Union's Horizon 2020 research and innovation programme (grant agreement No 666971).

Literature Cited

Allesina, S., and S. Tang. 2012. Stability criteria for complex ecosystems. Nature 483:205–208.

Arnoldi, J.-F., A. Bideault, M. Loreau, and B. Haegeman. 2018. How ecosystems recover from pulse perturbations: A theory of short- to long-term responses. Journal of Theoretical Biology 436:79–92.

Arnoldi, J.-F., B. Haegeman, T. Revilla, and M. Loreau. 2016*a*. Particularity of universal resilience patterns in complex networks. bioRxiv 056218.

Arnoldi, J.-F., M. Loreau, and B. Haegeman. 2016*b*. Resilience, reactivity and variability: A mathematical comparison of ecological stability measures. Journal of Theoretical Biology 389:47–59.

Barbier, M., J.-F. Arnoldi, G. Bunin, and M. Loreau. 2018. Generic assembly patterns in large ecological communities. Proceedings of the National Academy of Sciences 115:2156–2161.

Biroli, G., G. Bunin, and C. Cammarota. 2017. Marginally stable equilibria in critical ecosystems. arXiv 1710.03606.

Bunin, G. 2017. Ecological communities with Lotka-Volterra dynamics. Physical Review E 95:042414.

Campbell, V., G. Murphy, and T. N. Romanuk. 2011. Experimental design and the outcome and interpretation of diversity stability relations. Oikos 120:399–408.

Chalcraft, D. R. 2013. Changes in ecological stability across realistic biodiversity gradients depend on spatial scale. Global Ecology and Biogeography 22:19–28.

Donohue, I., H. Hillebrand, J. M. Montoya, O. L. Petchey, S. L. Pimm, M. S. Fowler, K. Healy, A. L. Jackson, M. Lurgi, D. McClean, N. E. O'Connor, E. J. O'Gorman, and Q. Yang. 2016. Navigating the complexity of ecological stability. Ecology Letters 19:1172–1185.

Elton, C. 1946. Competition and the structure of ecological communities. Journal of Animal Ecology 15:54–68.

Griffin, J. N., E. J. OGorman, M. C. Emmerson, S. R. Jenkins, A.-M. Klein, M. Loreau, and A. Symstad. 2009. Biodiversity and the stability of ecosystem functioning. Oxford University Press.

Grilli, J., M. Adorisio, S. Suweis, G. Barabs, J. R. Banavar, S. Allesina, and A. Maritan. 2017. Feasibility and coexistence of large ecological communities. Nature Communications 8.

Grimm, V., and C. Wissel. 1997. Babel, or the ecological stability discussions: An inventory and analysis of terminology and a guide for avoiding confusion. Oecologia 109:323–334.

Gross, T., L. Rudolf, S. A. Levin, and U. Dieckmann. 2009. Generalized models reveal stabilizing factors in food webs. Science 325:747–750.

Gurney, W., and R. M. Nisbet. 1998. Ecological Dynamics. Oxford University Press.

Haegeman, B., J.-F. Arnoldi, S. Wang, C. de Mazancourt, J. M. Montoya, and M. Loreau. 2016. Resilience, invariability, and ecological stability across levels of organization. bioRxiv 085852.

Haegeman, B., and M. Loreau. 2011. A mathematical synthesis of niche and neutral theories in community ecology. Journal of Theoretical Biology 269:150–165.

Hector, A., Y. Hautier, P. Saner, L. Wacker, R. Bagchi, J. Joshi, M. Scherer-Lorenzen, E. M. Spehn, E. Bazeley-White, M. Weilenmann, M. C. Caldeira, P. G. Dimitrakopoulos, J. A. Finn, K. Huss-Danell, A. Jumpponen, C. P. H. Mulder, C. Palmborg, J. S. Pereira, A. S. D. Siamantziouras, A. C. Terry, A. Y. Troumbis, B. Schmid, and M. Loreau. 2010. General stabilizing effects of plant diversity on grassland productivity through population asynchrony and overyielding. Ecology 91:2213–2220.

Hill, M. O. 1973. Diversity and evenness: a unifying notation and its consequences. Ecology 54:427–432.

Ives, A. R., and S. R. Carpenter. 2007. Stability and diversity of ecosystems. Science 317:58–62.

Jiang, L., and Z. Pu. 2009. Different effects of species diversity on temporal stability in single trophic and multitrophic communities. The American Naturalist 174:651–659.

Kilpatrick, A. M., and A. R. Ives. 2003. Species interactions can explain Taylor's power law for ecological time series. Nature 422:65–68.

Lande, R., S. Engen, and B.-E. Saether. 2003. Stochastic Population Dynamics in Ecology and Conservation. Oxford University Press.

Loreau, M., and C. de Mazancourt. 2013. Biodiversity and ecosystem stability: A synthesis of underlying mechanisms. Ecology Letters 16:106–115.

MacArthur, R. 1955. Fluctuations of animal populations and a measure of community stability. Ecology 36:533–536.

May, R. M. 1972. Will a large complex system be stable? Nature 238:413–414.

———. 1973. Stability and Complexity in Model Ecosystems. Princeton University Press.

McCann, K. S. 2000. The diversity-stability debate. Nature 405:228–233.

Pimm, S. L. 1984. The complexity and stability of ecosystems. Nature 307:321–326.

———. 1991. The Balance of Nature? Ecological Issues in the Conservation of Species and Communities. University of Chicago Press.

Roberts, A. 1974. The stability of a feasible random ecosystem. Nature 251:607–608.

Ruokolainen, L., and M. S. Fowler. 2008. Community extinction patterns in coloured environments. Proceedings of the Royal Society of London B: Biological Sciences 275:1775–1783.

Scheffer, M., J. Bascompte, W. A. Brock, V. Brovkin, S. R. Carpenter, V. Dakos, H. Held, E. H. van Nes, M. Rietkerk, and G. Sugihara. 2009. Early-warning signals for critical transitions. Nature 461:53–59.

Taylor, L. R. 1961. Aggregation, variance and the mean. Nature 189:732–735.

Tilman, D., P. B. Reich, and J. M. H. Knops. 2006. Biodiversity and ecosystem stability in a decade-long grassland experiment. Nature 441:629–632.

Tilman, D., D. Wedin, and J. Knops. 1996. Productivity and sustainability influenced by biodiversity in grassland ecosystems. Nature 379:718–720.

Van Kampen, N. G. 1997. Stochastic Processes in Physics and Chemistry. Elsevier.

Vasseur, D. A., and P. Yodzis. 2004. The color of environmental noise. Ecology 85:1146–1152.

Wang, S., and M. Loreau. 2014. Ecosystem stability in space: α, β and γ variability. Ecology Letters 17:891–901.

Wang, S., M. Loreau, J.-F. Arnoldi, J. Fang, K. A. Rahman, S. Tao, and C. d. Mazancourt. 2017. An invariability-area relationship sheds new light on the spatial scaling of ecological stability. Nature Communications 8:15211.

Yachi, S., and M. Loreau. 1999. Biodiversity and ecosystem productivity in a fluctuating environment: The insurance hypothesis. Proceedings of the National Academy of Sciences 96:1463–1468.

Zelnik, Y. R., J.-F. Arnoldi, and M. Loreau. 2018. The three regimes of spatial recovery. bioRxiv 308635 .

Appendix

The Appendix is organized as follows: Appendix A through D provides a self-contained presentation of the mathematical foundations of our variability theory. Appendix E through I provide details concerning specific applications considered in the main text: two-species communities in Appendix F, complex Lotka-Volterra communities in appendices F-G, the link between abundance statistics and variability in Appendix H and, finally, a study of two common population and ecosystem-level variability notions in Appendix I.

A Response to white-noise perturbation

We describe the response of a linear dynamical system, representing the dynamics of displacement of species around an equilibrium value, to a white-noise perturbation. Stochastic perturbations in continuous time are mathematically quite subtle. However, in the setting of linear dynamical systems, the effect of a white-noise perturbation can be analyzed relatively easily. Because this analysis is not readily available in the ecology literature, we present here a short overview. We start by from a fomulation in vector notation,

$$\frac{d\boldsymbol{x}}{dt} = A\boldsymbol{x} + \boldsymbol{\xi}(t), \tag{A1}$$

where $\boldsymbol{x} = (x_i)$ denotes the vector of species displacements, $\boldsymbol{\xi} = (\xi_i)$ the vector of species perturbations, and $A = (A_{ij})$ the community matrix.

Suppose that the perturbation $\boldsymbol{\xi}(t)$ consists in a sequence of pulses. We denote the times at which these pulses occur by t_k, and the corresponding pulse directions by $\boldsymbol{u}_k = (u_{k,i})$. The

multi-pulse perturbation can then be written as

$$\boldsymbol{\xi}(t) = \sum_k \delta(t - t_k)\, \boldsymbol{u}_k. \tag{A2}$$

where we have used the Dirac delta function $\delta(t)$.

We model both the pulse times t_k and the pulse directions $\boldsymbol{u}_k$ as random variables. Specifically, we assume that the pulse times are distributed according to a Poisson point process with intensity f. This means that the probability that a pulse occurs in a small time interval of length Δs is equal to $f\Delta s$, and that this occurrence is independent of any other model randomness. We denote the average over the pulse times t_k by $\mathbb{E}_f$.

Furthermore, we assume that the pulse directions $\boldsymbol{u}_k$ are independent (mutually independent, and independent of any other model randomness) and identically distributed. They have zero mean, and their second moments are given by the covariance matrix C_u. That is, denoting the average over the pulse directions $\boldsymbol{u}_k$ by $\mathbb{E}_u$, we have $\mathbb{E}_u\, u_{k,i} = 0$, $\mathbb{E}_u\, u_{k,i}^2 = C_{u,ii}$, $\mathbb{E}_u\, u_{k,i}u_{k,j} = C_{u,ij}$, and $\mathbb{E}_u\, u_{k,i}u_{\ell,i} = \mathbb{E}_u\, u_{k,i}u_{\ell,j} = 0$ for $i \neq j$ and $k \neq \ell$. The latter equations can be written in vector notation,

$$C_u = \mathbb{E}_u\, \boldsymbol{u}_k\boldsymbol{u}_k^\top \qquad \text{and} \qquad \mathbb{E}_u\, \boldsymbol{u}_k\boldsymbol{u}_\ell^\top = 0. \tag{A3}$$

We use this information to compute the statistics of species displacements $\boldsymbol{x}(t)$. Because the system response to a single pulse perturbation at time t_k in directon $\boldsymbol{u}_k$ is equal to $e^{(t-t_k)A}\boldsymbol{u}_k$, the system response to the sequence (A2) of pulse perturbations is equal to

$$\boldsymbol{x}(t) = \sum_{k|t_k<t} e^{(t-t_k)A}\, \boldsymbol{u}_k. \tag{A4}$$

Taking the mean over the perturbation directions, we obtain

$$\mathbb{E}_u\, \boldsymbol{x}(t) = \sum_{k|t_k<t} e^{(t-t_k)A}\, \mathbb{E}_u\, \boldsymbol{u}_k = 0,$$

showing that the species displacements fluctuate around the unperturbed equilibrium.

Next, we compute the covariance matrix of the species displacements,

$$C_x = \mathbb{E}_{f,u}\, \boldsymbol{x}(t)\boldsymbol{x}(t)^\top. \tag{A5}$$

We substitute the response to the multi-pulse perturbation, equation (A4),

$$\begin{aligned}
C_x &= \mathbb{E}_{f,u} \sum_{k|t_k<t} e^{(t-t_k)A}\, \boldsymbol{u}_k \sum_{\ell|t_\ell<t} \boldsymbol{u}_\ell^\top\, e^{(t-t_\ell)A^\top} \\
&= \mathbb{E}_f \sum_{k|t_k<t} \sum_{\ell|t_\ell<t} e^{(t-t_k)A}\, \mathbb{E}_u\, \boldsymbol{u}_k \boldsymbol{u}_\ell^\top\, e^{(t-t_\ell)A^\top} \\
&= \mathbb{E}_f \sum_{k|t_k<t} e^{(t-t_k)A}\, \mathbb{E}_u\, \boldsymbol{u}_k \boldsymbol{u}_k^\top\, e^{(t-t_k)A^\top} \\
&= \mathbb{E}_f \sum_{k|t_k<t} e^{(t-t_k)A}\, C_u\, e^{(t-t_k)A^\top},
\end{aligned}$$

where we have used equation (A3). To take the average over the pulse times, we partition the time axis in small intervals of length Δs. Writing $s_n = n\Delta s$ for any integer n, we get

$$C_x = \sum_{n|s_n<t} e^{(t-s_n)A}\, C_u\, e^{(t-s_n)A^\top} f\Delta s,$$

because the contribution of term n is equal to $e^{(t-s_n)A}\, C_u\, e^{(t-s_n)A^\top}$ with probability $f\Delta s$, and

zero otherwise. Assuming that the time intervals Δs are infinitesimal, we find the integral

$$\begin{aligned} C_x &= \int_{-\infty}^{t} e^{(t-s)A}\, C_u\, e^{(t-s)A^\top} f ds \\ &= \int_{0}^{\infty} e^{sA}\, C_u\, e^{sA^\top} f ds \\ &= \int_{0}^{\infty} e^{sA}\, \big(fC_u\big)\, e^{sA^\top} ds. \end{aligned} \tag{A6}$$

Hence, we have obtained the stationary covariance matrix of the species displacements under a stochastic multi-pulse perturbation.

A white-noise perturbation corresponds to a special case of the stochastic multi-pulse perturbation, namely, to the case of extremely frequent pulses (large f) of small size (small $\|\boldsymbol{u}\|$). More precisely, we have to take the coupled limit $f \to \infty$ and $C_u \to 0$ while keeping fC_u constant. Because equation (A6) depends on f and C_u through the product fC_u only, the same expression is also valid for white-noise perturbations.

Alternatively, the stationary covariance matrix C_x can be obtained by solving the so-called Lyapunov equation,

$$AC + CA^\top + E = 0, \tag{A7}$$

where E is the covariance matrix characterizing the white noise, equal to fC_u in our case. Indeed, it can be verified that equation (A6) satisfies equation (A7),

$$\begin{aligned} AC_x + C_xA^\top &= \int_0^\infty \Big(Ae^{sA}\, fC_u\, e^{sA^\top} ds + e^{sA}\, fC_u\, e^{sA^\top} A^\top\Big) ds \\ &= \int_0^\infty \frac{d}{ds}\Big(e^{sA}\, fC_u\, e^{sA^\top}\Big) ds \\ &= e^{sA}\, fC_u\, e^{sA^\top}\Big|_{s\to\infty} - e^{sA}\, fC_u\, e^{sA^\top}\Big|_{s=0} \\ &= -fC_u. \end{aligned}$$

For a stable matrix A this is the unique solution of the Lyapunov equation, for which we introduce the short-hand notation $\mathcal{L}(A, E)$,

$$\mathcal{L}(A, E) = \int_0^\infty e^{sA}\, E\, e^{sA^\top} ds. \tag{A8}$$

Hence, we can write

$$C_x = \mathcal{L}(A, fC_u), \tag{A9}$$

which is the notation used in the main text. From a numerical viewpoint, the covariance matrix C_x can be easily obtained by solving the Lyapunov equation (A7), which can be written as a system of S^2 linear equations, rather than by computing the integral in (A8). Note also that solution of Lyapunov equation is linear in the perturbation covariance matrix,

$$\mathcal{L}(A, c_1E_1 + c_2E_2) = c_1\, \mathcal{L}(A, E_1) + c_2\, \mathcal{L}(A, E_2). \tag{A10}$$

B Construction of variability measure

We explain the construction of the variability measure $\mathcal{V}(E)$. The construction is based on the comparison of the intensity of the system response relative to the intensity of the applied perturbation. It should be stressed that, while we take special care of quantifying these intensities in a reasonable way, alternative choices are possible.

Perturbation intensity A reasonable measure of the perturbation intensity should increase with the number of pulses and the intensity of each pulse separately. In particular, we expect it to be proportional to the pulse frequency f and to some function of the pulse covariance matrix C_u.

We propose to look at the squared displacements $\|\boldsymbol{u}_k\|^2$ induced by pulses $\boldsymbol{u}_k$. The accumulated squared displacement in time interval $[t, t+T]$ is

$$\sum_{t_k \in [t,t+T]} \|\boldsymbol{u_k}\|^2.$$

Taking the average over pulse times and pulse directions,

$$\mathbb{E}_{f,u} \sum_{t_k \in [t,t+T]} \|\boldsymbol{u_k}\|^2 = \sum_{n|t<s_n<t+T} \mathbb{E}_u \|\boldsymbol{u}\|^2 \, f \Delta s,$$

where we have partitioned the time axis in small intervals of length Δs (see derivation of equation (A6)). Then,

$$\mathbb{E}_{f,u} \sum_{t_k \in [t,t+T]} \|\boldsymbol{u_k}\|^2 = \mathrm{Tr}\big(C_u\big) f T.$$

The result is proportional to the length T of the considered time interval. The average accumulated squared displacement per unit of time is

$$\frac{1}{T} \, \mathbb{E}_{f,u} \sum_{t_k \in [t,t+T]} \|\boldsymbol{u_k}\|^2 = \mathrm{Tr}\big(f C_u\big). \tag{B1}$$

As expected, this quantity is proportional to the pulse frequency f and increases with the pulse covariance matrix C_u. Note also that f and C_u appear as a product, so that the expression is compatible with the white-noise limit.

Equation (B1) quantifies the intensity of the perturbation applied to the entire ecosystem. This measure is not directly appropriate to normalize the pertubation intensity across systems. Indeed, when keeping the total perturbation intensity constant, the perturbation applied to a given species would be weaker in a community with a larger number of species. To eliminate this artefact, we normalize the perturbation intensity on a per species basis. Thus, we propose

to quantify the perturbation intensity as

$$\sigma_{\text{in}}^2 = \frac{f}{S} \operatorname{Tr} C_u. \tag{B2}$$

Response intensity We measure the intensity of the system response in terms of the covariance matrix C_x. This matrix encodes the statistical properties of the biomass fluctuations in stationary state. For example, species biomass $x_i(t)$ fluctuates around its equilibrium value N_i with variance $C_{x,ii}$. More generally, we can describe the fluctuations of any function φ of species biomasses. The dynamics near equilibrium are

$$\varphi(\boldsymbol{n}(t)) = \varphi(\boldsymbol{N}) + \boldsymbol{v}^\top \boldsymbol{x}(t),$$

where vector $\boldsymbol{v} = \nabla\varphi$ is the gradient of the function φ evaluated at the equilibrium $\boldsymbol{N}$. This vector gives the direction in which the system fluctuations are observed. Then, denoting the temporal mean and variance by $\mathbb{E}_t$ and Var_t, we have

$$\begin{aligned}
\mathrm{Var}_t\left(\varphi(\boldsymbol{n}(t))\right) &= \mathbb{E}_t\Big(\big(\boldsymbol{v}^\top \boldsymbol{x}(t)\big)^2\Big) \\
&= \mathbb{E}_t\Big(\boldsymbol{v}^\top \boldsymbol{x}(t)\boldsymbol{x}(t)^\top \boldsymbol{v}\Big) \\
&= \boldsymbol{v}^\top \mathbb{E}_t\big(\boldsymbol{x}(t)\boldsymbol{x}(t)^\top\big)\boldsymbol{v} \\
&= \boldsymbol{v}^\top C_x\, \boldsymbol{v}.
\end{aligned} \tag{B3}$$

We use this variance to quantify the intensity of the system response. Rather than choosing a particular vector $\boldsymbol{v}$, we consider the average over all observation directions. Specifically, we restrict attention to unit vectors $\boldsymbol{v}$ and average over the uniform distribution of such vectors.

Denoting this average by $\mathbb{E}_v$, we get

$$\mathbb{E}_v \operatorname{Var}_t\big(\varphi(\boldsymbol{n}(t)\big) = \mathbb{E}_v \left(\boldsymbol{v}^\top C_x \boldsymbol{v}\right) = \operatorname{Tr} \mathbb{E}_v \, \boldsymbol{v}\boldsymbol{v}^\top C_x.$$

It follows from species symmetry that the average $\mathbb{E}_v \, \boldsymbol{v}\boldsymbol{v}^\top$ is proportional to the unit matrix. Moreover, because $\operatorname{Tr} \boldsymbol{v}\boldsymbol{v}^\top = 1$ for all vectors $\boldsymbol{v}$, the constant of proportionality is equal to $\frac{1}{S}$. Hence,

$$\mathbb{E}_v \operatorname{Var}_t\big(\varphi(\boldsymbol{n}(t)\big) = \frac{1}{S} \operatorname{Tr} C_x.$$

Therefore, we propose to quantify the response intensity as

$$\sigma^2_{\text{out}} = \frac{1}{S} \operatorname{Tr} C_x. \tag{B4}$$

Variability and invariability We define variability $\mathcal{V}$ as the ratio of the response intensity σ^2_{out} and the perturbation intensity σ^2_{in},

$$\mathcal{V} = \frac{\sigma^2_{\text{out}}}{\sigma^2_{\text{in}}} = \frac{\frac{1}{S} \operatorname{Tr} C_x}{\frac{f}{S} \operatorname{Tr} C_u} = \frac{\operatorname{Tr} C_x}{f \operatorname{Tr} C_u}.$$

Substituting equation (A9) for C_x, we get

$$\mathcal{V} = \frac{\operatorname{Tr} \mathcal{L}(A, f C_u)}{f \operatorname{Tr} C_u} = \operatorname{Tr} \mathcal{L}\big(A, \frac{C_u}{\operatorname{Tr} C_u}\big),$$

where we have used the linearity property (A10). We see that only the normalized perturbation covariance matrix matters in this expression. That is, the variability measure focuses on the directional effect of the perturbation. We make this dependence explicit in the notation, and write

$$\mathcal{V}(E) = \operatorname{Tr} \mathcal{L}(A, E), \tag{B5}$$

where $E = \frac{C_u}{\operatorname{Tr} C_u}$ is the perturbation direction, i.e., a covariance matrix with unit trace.

Variability is inversely related to stability: the more variable an ecosytem, the less stable it is. For purpose of comparison, we construct a stability measure based on variability $\mathcal{V}(E)$, which we call invariability $\mathcal{I}(E)$,

$$\mathcal{I}(E) = \frac{1}{2\,\mathcal{V}(E)}. \tag{B6}$$

The factor 2 in this definition guarantees that we recover asymptotic resilience for the simplest dynamical systems. To see this, consider a system of S non-interacting species, in which all species have the same return rate λ. The community matrix is equal to $A = -\lambda \mathbb{1}$ where $\mathbb{1}$ denotes the identity matrix. From the Lyapunov equation (A7) we get the stationary covariance matrix $\mathcal{L}(A, E) = \frac{1}{2\lambda} E$. Therefore, $\mathcal{V}(E) = \frac{1}{2\lambda}$ and $\mathcal{I}(E) = \lambda$, which is equal to the asymptotic resilience of this example system.

C Worst-case and mean-case variability

Worst-case variability is defined as

$$\mathcal{V}^{\text{worst}} = \max_E \mathcal{V}(E) = \max_E \operatorname{Tr} \mathcal{L}(A, E) \tag{C1}$$

where the maximum is taken over perturbation directions, i.e., over covariance matrices E with $\operatorname{Tr} E = 1$. The function $\operatorname{Tr} \mathcal{L}(A, E)$ is linear in the perturbation direction E, see equation (A10), and the set of perturbation directions is convex. Hence, the maximum is reached at an extreme point, that is, on the boundary of the set. The extreme points are the purely directional perturbations (see Appendix E for the argument in the two-species case), so that the maximum is reached at a purely directional perturbation. Arnoldi et al. (2016*b*) showed that the worst-case variability can be easily computed, namely, as a specific norm of the

operator $\widehat{A}^{-1}$ that maps E to $\mathcal{L}(A, E)$. Concretely

$$\widehat{A} = A \otimes \mathbb{1} + \mathbb{1} \otimes A, \tag{C2}$$

so that

$$\mathcal{V}^{\text{worst}} = ||\widehat{A}^{-1}||, \tag{C3}$$

where $|| \cdot ||$ stands for the spectral norm of $S^2 \times S^2$ matrices.

To define **mean-case variability** $\mathcal{V}^{\text{mean}}$, we assume a probability distribution over the perturbation directions, and compute the mean system response over this distribution. Due to the linearity property (A10), this mean response is equal to the response to the mean perturbation direction. Hence, we do not have to specify the full probability distribution over the perturbation directions; it suffices to determine the mean perturbation direction. As can be directly verified in the two-species case (Appendix E), if, averaged over the distribution of perturbation directions, perturbation intensities are evenly distributed across species, and positive and negative correlations between species perturbations cancel out, then the mean perturbation direction is adirectional. This corresponds to the center of the set of perturbation directions (the disc center in the two-species case), and is proportional to the identity matrix, that is, $E = \frac{1}{S}\mathbb{1}$. Therefore,

$$\mathcal{V}^{\text{mean}} = \operatorname{Tr} \mathcal{L}(A, \tfrac{1}{S}\mathbb{1}). \tag{C4}$$

D Perturbation types and variability

The perturbation type (environmental-, demographic- or immigration-type) affects how the perturbation intensity is distributed across species. Therefore, it also affects our measure of variability, as defined in Appendix B. Here we describe how the variability definition has to

be modified.

We defined variability measure (B5) as the intensity of the system response relative to the intensity of the applied perturbation. To quantify the perturbation intensity in the case of biomass-dependent perturbations, we distinguish the intrinsic effect of the perturbation on a species, which does not depend on the species' biomass, and the total effect of the perturbation on the species, which does depend on biomass. We propose to express the perturbation intensity in terms of the intrinsic perturbation, while it is the total perturbation that acts on the species dynamics.

Formally, for species i, we denote the intrinsic perturbation by $\xi_i^{\text{intr}}(t)$ and the total perturbation by $\xi_i^{\text{tot}}(t)$. Then, for a type-α perturbation, we have

$$\xi_i^{\text{tot}}(t) = N_i^{\frac{\alpha}{2}}\, \xi_i^{\text{intr}}(t), \tag{D1}$$

where N_i is the biomass of species i. Thus, the intrinsic perturbation $\xi^{\text{intr}}(t)$ can be interpreted as the perturbation per unit of biomass. Equation (D1) can be written in vector notation as

$$\boldsymbol{\xi}^{\text{tot}}(t) = D^{\frac{\alpha}{2}} \boldsymbol{\xi}^{\text{intr}}(t), \tag{D2}$$

where D is the diagonal matrix whose entries are species equilibrium biomass ($D_{ii} = N_i$).

Both the intrinsic and total perturbation are multi-pulse. If we denote the pulses of the intrinsic perturbation by $\boldsymbol{u}_k$, then, by equation (D2), those of the total perturbation are $D^{\alpha}\boldsymbol{u}_k$. Then, to quantify the perturbation intensity, we use the covariance matrix of the pulses in the intrinsic perturbation. Repeating the derivation leading to equation (B2), we have

$$\sigma_{\text{in}}^2 = \frac{1}{S}\text{Tr}\big(fC_u\big). \tag{D3}$$

However, to compute the covariance matrix of the species displacements, we use the covariance matrix of the pulses in the total perturbation. This corresponds to replacing C_u by $D^{\frac{\alpha}{2}} C_u D^{\frac{\alpha}{2}}$ in the derivation of equation (B4), so that we get

$$\sigma^2_{\text{out}} = \frac{1}{S} \text{Tr}\, \mathcal{L}\big(A, f D^{\frac{\alpha}{2}} C_u D^{\frac{\alpha}{2}}\big). \tag{D4}$$

The variability measure for a type-α perturbation becomes

$$\mathcal{V}_\alpha = \frac{\sigma^2_{\text{out}}}{\sigma^2_{\text{in}}} = \text{Tr}\, \mathcal{L}\big(A, \frac{D^{\frac{\alpha}{2}} C_u D^{\frac{\alpha}{2}}}{\text{Tr}\, C_u}\big),$$

or, in terms of the (intrinsic) perturbation direction E,

$$\mathcal{V}_\alpha(E) = \text{Tr}\, \mathcal{L}\big(A, D^{\frac{\alpha}{2}} E D^{\frac{\alpha}{2}}\big). \tag{D5}$$

Applying the same arguments as in Appendix C), we find that worst-case variability,

$$\mathcal{V}^{\text{worst}}_\alpha = \max_E \mathcal{V}_\alpha(E) = \max_E \ \text{Tr}\, \mathcal{L}\big(A, D^{\frac{\alpha}{2}} E D^{\frac{\alpha}{2}}\big),$$

is attained at a perfectly correlated perturbation. If we define the operator (an $S^2 \times S^2$ matrix)

$$\mathcal{D}_\alpha = D^{\frac{\alpha}{2}} \otimes D^{\frac{\alpha}{2}},$$

then the worst case-variability can be computed as

$$\mathcal{V}^{\text{worst}}_\alpha = ||\widehat{A}^{-1} \circ \mathcal{D}_\alpha||, \tag{D6}$$

where $||\cdot||$ is the spectral norm for $S^2 \times S^2$ matrices. On the other hand, the mean-case

variability,

$$\mathcal{V}_\alpha^{\text{mean}} = \operatorname{Tr} \mathcal{L}\big(A, \tfrac{1}{S} D^\alpha\big), \tag{D7}$$

is attained by the uniform, uncorrelated perturbation.

E Perturbation directions in two dimensions

Variability spectra are built on the notion of perturbation directions. They are characterized by a covariance matrix E with $\operatorname{Tr} E = 1$. To gain some intuition, we study the set of perturbation directions in the case of two species.

Any perturbation direction E in two dimensions can be written as

$$E = \begin{pmatrix} 1-x & y \\ y & x \end{pmatrix}. \tag{E1}$$

with $0 \leq x \leq 1$ and $y^2 \leq x(1-x)$. The first inequality guarantees that the elements on the diagonal are variances, i.e., positive numbers. The second inequality guarantees that the off-diagonal element is a proper covariance, in particular, that the correlation coefficient is contained between -1 and 1. Note also that matrix (E1) has always $\operatorname{Tr} E = 1$.

It follows from equation (E1) that the set of perturbation directions in two dimensions is parameterized by two numbers x and y. Using these numbers as axes of a two-dimensional plot, we see that the set of perturbation directions corresponds to a disc with radius 0.5 and centered at $(0.5, 0)$ (cf. Fig. 3).

It is instructive to study the position of specific perturbation directions on the disc. The point $(0, 0)$ corresponds to a perturbation affecting only the first species, whereas point $(1, 0)$ is a perturbation only affecting the second species. More generally, any point on the boundary

of the disc correspond to a multi-pulse perturbation for which the individual pulses have a fixed direction. For example, the point $(0.5, 0.5)$ is a perturbation for which each pulse has the same effect on species 1 and species 2, whereas the perturbation corresponding to point $(0.5, -0.5)$ consists of pulses that affect the two species equally strongly, but in an opposite way. Perturbations on the boundary are *perfectly correlated*.

The perturbations towards the center of the disc are composed of pulses with more variable directions. For example, a multi-pulse perturbation for which half of the pulses affect only the second species, and the other pulses affect the two species equally strongly corresponds to the point $\frac{1}{2}(0, 1) + \frac{1}{2}(0.5, 0.5) = (0.25, 0.75)$. The mixture of different pulse directions is the strongest at the center of the disc $(0.5, 0)$. Examples of ways to realize this perturbation are $\frac{1}{2}(0, 0) + \frac{1}{2}(1, 0)$, $\frac{1}{2}(0.5, 0.5) + \frac{1}{2}(0.5, -0.5)$ and $\frac{1}{4}(0, 0) + \frac{1}{4}(0.5, 0.5) + \frac{1}{4}(1, 0) + \frac{1}{4}(0.5, -0.5)$. In each of these example, the pulses have their intensities, averaged over time, evenly distributed across species, and affect them, again averaged over time, in an uncorrelated way. The perturbation corresponding to the point $(0.5, 0)$ is thus evenly distributed across species but uncorrelated in time.

F Random Lotka-Volterra model

Consider a pool of species following random Lotka-Volterra interactions

$$\frac{dN_i(t)}{dt} = \frac{r_i N_i(t)}{K_i} \left(K_i - N_i(t) - \sum_{j \,|\, j \rightsquigarrow i}^{S_{\text{pool}}} B_{ij} N_j(t) \right); \quad i = 1, ..., S_{\text{pool}} \tag{F1}$$

and let the dynamics settle to an equilibrium community of S remaining species. In the above equation, the fact that species j has an effect of species i is noted as $j \rightsquigarrow i$. We fixed the network connectance of $\frac{1}{2}$, so that species interact, on average, with half of the

pool. By gradually increasing the size of the pool and drawing random parameters –growth rates r_i, carrying capacities K_i, and interaction strengths B_{ij}– we generated many different communities of various diversity. We consider a single trophic level, representing unstructured, mostly competitive, communities. The mean interaction strength is set to 0.1 and its standard deviation to 0.1, thus allowing some occasional positive interactions (e.g. facilitation). Growth rates and carrying capacities are independently drawn from a normal distribution of unit mean and 0.2 standard deviation.

Increasing the size of the pool from one species to one hundred we generated communities of various realized diversity. We repeated the process until we had 50 communities for each value of realized diversity, from 1 to 30. For each realization of the random community, and a given perturbation type we then generated 1000 random perturbations leading to 1000 values of variability. From each variability distribution we extracted its mean, its first and second quartile, its maximum and minimum values. From the communities we computed asymptotic resilience, worst-case variability and the prediction for the mean. Then we computed the median of these statistics and predictions over the set of 50 realizations per values of diversity, leading to Fig. 6.

G Limit of strong interactions

We give some elements as to why the behavior reported in Figs. 4 and 5 in the main text can be expected to be a general trend in diverse communities of interacting species. For that purpose, consider the Lotka-Volterra dynamics (F1), from the perspective of a focal species (of index 0). If a stable equilibrium exists in which the focal species survives at abundance

N_0, displacements from equilibrium $x_i = N_i(t) - N_i$ will be met with the dynamics

$$\frac{dx_0}{dt} = -\frac{x_0 + \sum_j B_{0j} x_j}{\tau_0} \; ; \quad \tau_0 = \frac{K_0}{r_0 N_0}. \tag{G1}$$

In this expression τ_0 sets the characteristic time scale of the focal species dynamics. This species-specific time scale is directly related to the species' contribution to variability. Indeed, the slower the species, the larger the impact of a repeated perturbation acting on this species, and the larger the species' contribution to variability (see also Discussion).

Without interactions, we have $N_0 = K_0$ and therefore $\tau_0 = 1/r_0$. In this case the time scale of that species dynamics is set by the inverse of its growth rate, *a priori* unrelated to its abundance K_0. This is the case in the example on the first row of Fig. 5, in which we drew growth rates and carrying capacities independently. Alternatively, we could assume some trade-off between growth rates and carrying capacities, causing low abundance to be associated with lower contribution to variability, illustrated on the second row of Fig. 5. In other words, without interactions, there is no clear relationship to be expected between abundance of perturbed species and variability.

If species interact, however, the focal species equilibrium abundance will satisfy

$$N_0 = K_0 + \sum_j B_{0j} N_j, \tag{G2}$$

where the sum measures the contribution of all other species. This term involves potentially very indirect effects between species. Other surviving species satisfy similar conditions so that

$$N_0 = K_0 + \sum_j B_{0j} K_j + \sum_{j,k} B_{0j} B_{jk} K_k + \sum_{j,k,l} B_{0j} B_{jk} B_{kl} K_l + \dots \tag{G3}$$

where we see direct interactions $j \rightsquigarrow 0$ (B_{0j}) but also indirect effects $k \rightsquigarrow j \rightsquigarrow 0$ ($B_{0j}B_{jk}$) and so on. Hence, if the overall interactions with all other species plays a preponderant role in determining the focal species abundance, then the carrying capacity K_0 will not control N_0. Hence, the characteristic time scale τ_0 of the focal species can become inversely proportional to its abundance N_0. If this is the case, more abundant species have faster dynamics and generate a smaller response if perturbed independently of their abundance, that is, if the perturbation is of the immigration type ($\alpha = 0$). This explains the relationship between abundance and variability shown in the leftmost panel of Fig. 4. If perturbation intensity depends on species abundance, in the case of demographic-type ($\alpha = 1$) or environmental-type ($\alpha = 2$) perturbations, we obtain the relationships shown in the other two panels of Fig. 4. In summary, if species interactions are sufficiently strong and heterogeneous, we expect clear relationships between abundance of perturbed species and community variability.

H Variability and abundance statistics

From the observed relationship between abundance and variability (Figs. 4 and 5), patterns for worst- and mean-case variability can be deduced. This reveals a connection between stability and diversity metrics.

Conisder the variability $\mathcal{V}_\alpha^{\text{spec } i}$ caused by a perturbation of type α, fully focused on species i. In communities with strong and heterogeneous interactions (Appendix G) we have that

$$\mathcal{V}_\alpha^{\text{spec } i} \propto \underbrace{N_i^\alpha}_{\text{perturbation}} \times \underbrace{N_i^{-1}}_{\text{response}} = N_i^{\alpha-1}.$$

For immigration-type perturbations ($\alpha = 0$), worst-case variability is approached by taking

the maximum over species which gives

$$\mathcal{V}_{\alpha=0}^{\text{worst}} \approx \max_i \mathcal{V}_{\alpha=0}^{\text{spec } i} \propto \frac{1}{\min_i N_i}. \tag{H1}$$

so that worst-case variability is governed by the rarest species. Furthermore, the abundance of the rarest species typically decreases with diversity, so that the corresponding diversity-stability relationship is decreasing. For mean-case variability we get

$$\mathcal{V}_{\alpha=0}^{\text{mean}} = \frac{1}{S} \sum_i \mathcal{V}_{\alpha=0}^{\text{spec } i} \propto \frac{1}{S} \sum_i \frac{1}{N_i} = \langle N \rangle_{\text{harm}}^{-1}, \tag{H2}$$

where $\langle N \rangle_{\text{harm}}$ stands for the harmonic mean of species abundances. Mean abundance typically decreases with diversity, so that the corresponding diversity-stability relationship is decreasing.

When caused by environmental-type perturbations ($\alpha = 2$), variability is proportional to the abundance of the perturbed species, so that the worst case is approached by taking the maximum over species, giving

$$\mathcal{V}_{\alpha=2}^{\text{worst}} \approx \max_i \mathcal{V}_{\alpha=0}^{\text{spec } i} \propto \max_i N_i. \tag{H3}$$

so that worst-case invariability is governed by the most abundant species. For mean-case variability, averaging over species individual contributions, we get

$$\mathcal{V}_{\alpha=2}^{\text{mean}} \propto \frac{1}{S} \sum_i N_i = \langle N \rangle_{\text{arith}}, \tag{H4}$$

the arithmetic mean of species abundances. Mean abundance typically decreases with diversity, so that the corresponding diversity-stability relationship is increasing.

Note, that when caused by demographic-type perturbations ($\alpha = 1$) the species-by-species approach does not work: demographic variability probes a purely collective property of the community.

I Population- and ecosystem-level stability

In this appendix we revisit the diversity-stability relationships reported in Fig. 6. Instead of using average variance, eq. (3), to define variability, as we did so far, let us consider two measures that have been proposed to quantify stability at the ecosystem and at the population level. The first one, $\mathcal{I}^{\text{eco}}$, is simply the inverse CV of total biomass N_{tot}. The second, $\mathcal{I}^{\text{pop}}$, is the inverse weighted mean CV of species biomass. More precisely if $p_i = N_i/N_{tot}$, we define

$$\mathcal{I}^{\text{eco}} = \frac{1}{\text{CV}^2(N_{tot})}; \;\; \mathcal{I}^{\text{pop}} = \frac{1}{\left(\sum_i p_i \text{CV}(N_i)\right)^2}. \tag{I1}$$

On the top row of Fig. I1 we see that $\mathcal{I}^{\text{eco}}$ increases with diversity for all perturbation types. On the bottom row we see that $\mathcal{I}^{\text{pop}}$ decreases with diversity for all perturbation types.

By construction, regardless of perturbation type, $\mathcal{I}^{\text{eco}}$ gives a predominant weight to abundant species while also allowing for buffering effects driven by synchrony between species time-series (Loreau and de Mazancourt, 2013). On the other hand, regardless of perturbation type, $\mathcal{I}^{\text{pop}}$ gives a large weight to rare species.

In fact, along any environmental gradient $\mathcal{I}^{\text{pop}}$ detects transcritical bifurcations, i.e. goes to zero whenever a species gradually becomes extinct (Haegeman and Loreau, 2011). In this sense it is clearly sensitive to the presence of rare species. On the other hand, $\mathcal{I}^{\text{eco}}$ relates to the variability of total biomass which, by construction gives more weight to abundant species than to rare ones, but is also known to be a very specific direction in phase-space. Indeed,

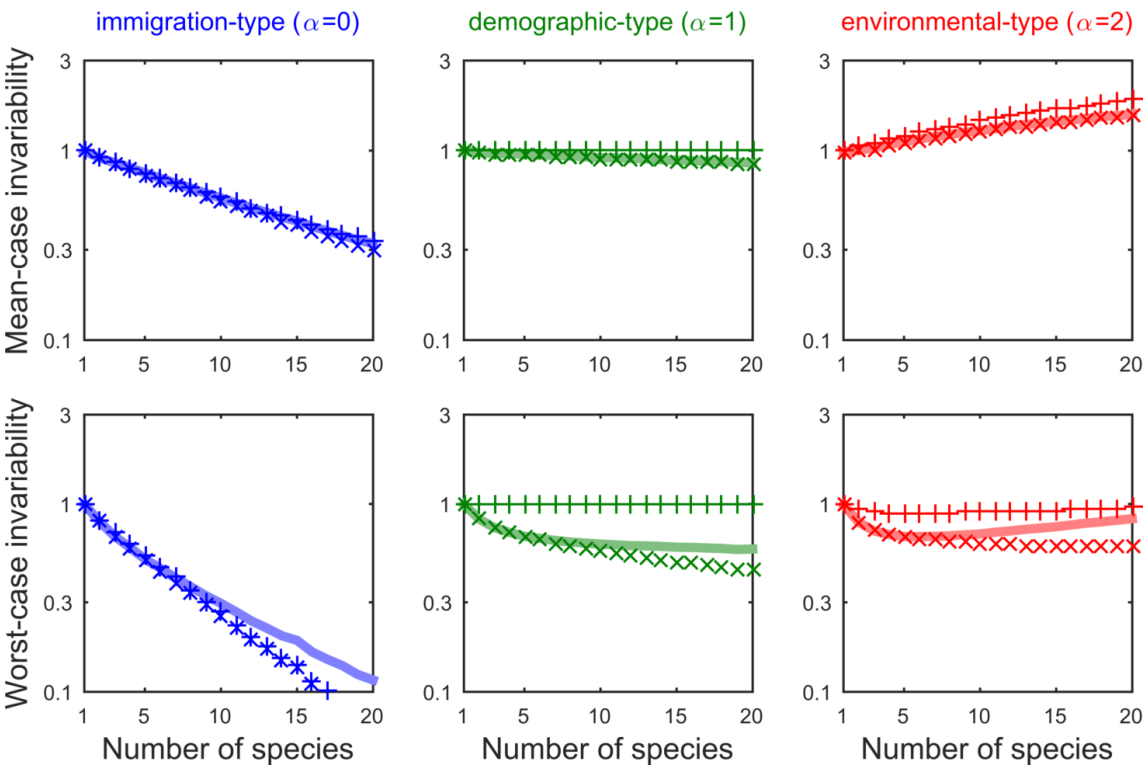

Figure H1: Invariability and species abundance. Top row: mean-case, bottom row: worst-case. x-marks: analytical formula; +-marks: approximation in terms of abundance (see Appendix H); thick line: simulation results. For immigration-type perturbations (first column, in blue), because each species contributes to variability proportionally to the inverse of its abundance, mean-case invariability scales as the harmonic mean abundance (eq. H2), which decreases with diversity. Worst-case invariability scales as the abundance of the rarest species. On the other hand, in response to environmental-type perturbations (third column, in red), mean-case variability scales as the arithmetic mean abundance (eq. H4) so that invariability increases. Worst case variability scales as the abundance of the most common species. In between (second column, in green), for demographic-type perturbations, neither worst- nor mean-case invariability is determined by statistics of species abundances.

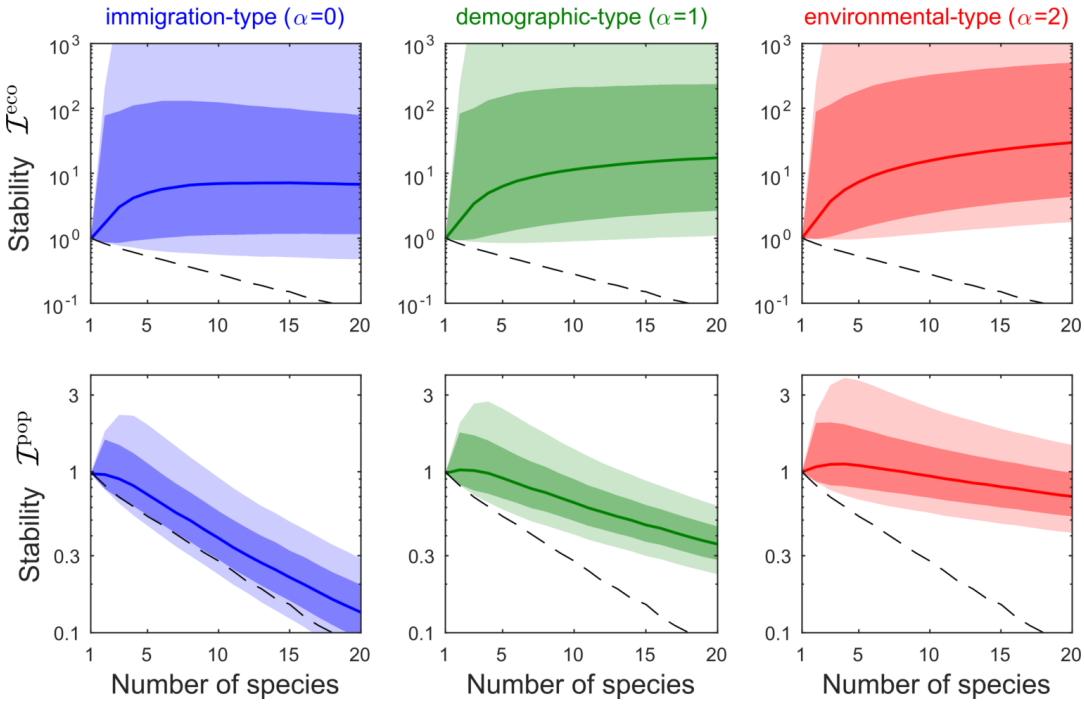

Figure I1: The choice of observation variable strongly affects the diversity-stability patterns. Same as Fig. 6, but instead of quantifying stability via average variance, we consider two stability measure that have been proposed to quantify invariability at the ecosystem and at the population level. The dashed line follows asymptotic resilience. Top row: invariability measure $\mathcal{I}^{\text{eco}}$ increases with diversity for all perturbation types. Bottom row: invariability measure $\mathcal{I}^{\text{pop}}$ decreases with diversity for all perturbation types.

for competitive systems, due to species compensation, it is the most stable directions, i.e. the direction along which perturbations are absorbed the fastest (Allesina and Tang, 2012; Arnoldi et al., 2016*a*). This effect was not present in the measure used in the main text, i.e. average variance, seen as the outcome of a random sampling over directions of observations (see Appendix B).

We see here the strong effect that the choice of observation can have on variability patterns, due to emphasis it puts on specific species abundance classes.